



Landslide prediction with severity analysis using efficient computer vision and soft computing algorithms

Payal Varangaonkar¹ · S. V. Rode²

Received: 26 September 2023 / Revised: 21 March 2024 / Accepted: 15 May 2024

© The Author(s), under exclusive licence to Springer Science+Business Media, LLC, part of Springer Nature 2024

Abstract

Since the preceding decade, there has been a great deal of interest in forecasting landslides using remote-sensing images. Early detection of possible landslide zones will help to save lives and money. However, this approach presents several obstacles. Computer vision systems must be carefully built since normal image processing does not apply to images obtained by remote sensing (RS). This research proposes a novel landslide prediction method with a severity analysis model based on real-time hyperspectral RS images. The proposed model consists of phases of pre-processing, dynamic segmentation, hybrid feature extraction, landslide prediction, and landslide severity detection. The pre-processing step performs the geometric correction of input RS images to suppress the built-up regions, water, and vegetation using the Normal Difference Vegetation Index (NDVI). The pre-processing stage encompasses many steps, including atmospheric adjustments, geometric corrections, and the elimination of superfluous regions by denoising techniques such as 2D median filtering. Dynamic segmentation is employed to segment the pre-processed picture for Region of Interest (ROI) localization. The ROI image is utilized to extract manually designed features that accurately depict spatial and temporal variations within the input RS image. For each input RS image, the hybrid feature vector is normalized. We trained ANN and SVM to predict landslides. If the input image predicts a landslide, its severity is identified. For the performance analysis, we collected real-time RS images of the western region of India (Goa and Maharashtra). Simulation results show the efficiency of the proposed model.

Keywords Computer vision methods · Classifications · Landslide detection · Normal digital vegetation index · Segmentation · Severity analysis · Western region

✉ Payal Varangaonkar
payal.varangaonkar@gmail.com
S. V. Rode
sandeepode30@gmail.com

¹ Sipna College of Engineering and Technology, Amravati, India

² Electronics and Telecommunication Department, Sipna College of Engineering & Technology, Amravati, India

1 Introduction

Landslides are one of the deadliest natural catastrophes in the world, damaging not only expensive houses and infrastructures but also inflicting a large number of casualties. Landslides have occurred throughout the world over the years, necessitating a thorough investigation [1]. According to David Petley's figures from the International Landslide Center at Durham University in the United Kingdom, there were roughly 2,620 fatal landslide occurrences worldwide between 2004 and 2010, killing a total of 32,322 persons [2]. In contrast to other parts of the world, Asia has a comparatively high number of landslides. Between 1950 and 2009, landslides killed over 18,000 individuals and impacted approximately 5.5 million people throughout Asia (EM-DAT 2010). The International Landslide Center at Durham University estimated in 2007 that China was the most severely afflicted country, with 695 landslide-related deaths, followed by India (352), Indonesia (465), Bangladesh (150), Vietnam (130), Nepal (168) [3]. In Asia, several landslides are happening in the Himalayas and Vietnam (my study regions), particularly after high rains, resulting in the loss of human lives and the destruction of property and infrastructure. Landslide threats can be avoided by utilizing remedial measures such as retaining walls, and anchor systems, lowering slope steepness, covering slopes with steel networks, and so on.

Additional measures to avoid landslides encompass: (1) reducing the amount of weight on steep inclines, (2) preventing the elevation of groundwater in slope-forming substances, (3) enveloping unstable slopes with impermeable membranes, and so on. However, these methods are only applicable to specific and localized slopes or small areas of unstable slopes. The mitigation of landslide occurrences at a regional level may be achieved by effective land use planning and decision-making, alongside the implementation of early warning systems. Landslide hazard assessment and mapping are commonly used to identify high-danger landslide areas. Remote Sensing (RS) and Geographic Information Systems (GIS) are increasingly recognized as crucial tools for researching landslide hazards [4–7]. GIS is a robust software application for geographical analysis, equipped with advanced tools for visual image processing and spatial data management. GIS is employed to integrate and oversee many forms of landslide data. The integration of RS methodologies with GIS enables a diverse array of functions for landslide monitoring and modeling, encompassing data collection, analysis, evaluation, and visualization. In recent years, there has been a significant development of GIS-based systems for landslide hazard modeling. These systems utilize several machine learning techniques, including Fuzzy Logic [8, 9], Neuro-Fuzzy [10–12], Artificial Neural Networks (ANN) [13–15], Support Vector Machines (SVM) [16, 17], and Decision-Tree Models [18, 19]. Numerous studies [20] have utilized RS photos to forecast, detect, or localize landslides by employing diverse image processing techniques and machine learning algorithms. A range of methodologies, including thresholding, binary temporal techniques, texture analysis, and others, were employed to conduct change detection using before and post-landslide photos. Nevertheless, these systems encountered significant challenges in terms of scalability, accuracy, and efficiency due to the incompatibility between the techniques employed for analyzing regular photographs and RS images.

Over the past decade, there has been significant interest in predicting landslides using RS photos due to its utilization of real-time visual data. Nevertheless, it has encountered various obstacles, such as inadequate data and information regarding landslide regions, specifically in western and northern India, inadequate methods for analyzing landslide images, low accuracy in assessing landslide changes, and intricate determination of

landslide change localization, among other challenges. Moreover, due to the intricate nature of natural phenomena, it is challenging to identify spatial patterns that are only associated with landslides. Consequently, attempting to forecast and locate landslides using artificial features or spatial data leads to unsatisfactory outcomes. Some recent research provided a thresholding strategy for autonomous landslide identification, although the accuracy of landslide detection is relatively low. There has been no published effort that addresses the challenge of landslide analysis with improved prediction accuracy. Several methods have recently been proposed for the landslide detection, but such methods suffered from the research problems described below.

- Deep learning solved several pattern recognition problems. This work invalidates such approaches because of their complexity and inability to reduce RS image pre-processing difficulties, which hinders quick prediction and localization.
- Scalability and accuracy issues plagued the current study because of its small datasets. Most of the works were from China, hence Indian landslide databases and studies were few. Scalable landslide datasets are scarce in western India.
- The lack of geometric rectification and quality enhancement of input RS photos increases prediction errors in current methods.
- Inaccurate landslide appraisal, poor image analysis, and problematic landslide change localization, among other issues.
- None of the existing works possess the capability to forecast landslides or estimate their severity.

These problems motivate us to present the novel landslide prediction mechanism in this study. The major focus of this research is on developing a framework for early-stage landslide prediction with improved accuracy. We present a novel semi-automatic framework proposed for landslide prediction and severity analysis using efficient computer vision and soft computing techniques. We build the real-time RS images dataset in this paper collected from the landslide regions of the western region of India (Goa and Maharashtra States). The RS images are collected for normal and landslide regions in the Goa and Maharashtra states. Once the dataset is built, the proposed model is designed and consists of steps such as pre-processing, dynamic segmentation, hybrid features extraction, prediction, and severity analysis. The novelty of the proposed model is described below.

- To expedite and anticipate the occurrence of landslide zones, a novel framework is introduced that employs straightforward but efficient computer vision techniques in conjunction with soft computing algorithms.
- The scalable dataset, consisting of over 2700 samples, was created from the western part of India, specifically the Maharashtra (Konkan landslide regions) and Goa landslide regions. The researchers utilized the Linear Imaging Self Scanning (LISS-3) satellite, specifically the Bhuvan satellite, to gather remote sensing (RS) photos of both landslides and non-landslides.
- The suggested technique for image pre-processing in RS aims to rectify geometric and atmospheric information, as well as eliminate noisy components.
- To enhance the precision of landslide image analysis and prediction, we employ a dynamic technique to segment each pre-processed RS image and extract the diverse handmade characteristics.

The remainder of this paper consists of the following sections. Section 2 describes the related works on landslide prediction. Section 3 presented the detailed methodology of this paper. Section 4 presented the simulation results and analysis. Section 5 presented the conclusion and suggestions.

2 Related works

This section provides a concise overview of the current methodologies utilizing machine learning techniques to predict landslides. The landslide prediction systems mostly relied on inputs such as GIS and RS data. These studies explore the core functionality and steps of processing the real-time RS images.

2.1 State-of-the-arts

The approach for forecasting landslides using optical satellite pictures was invented by [21]. The dataset was collected utilizing RS image settings with a high resolution of 5 m, a posting distance of 30 m, and a coarse interpretation. The utilization of multi-temporal sensor pictures for change detection, based on radio-metric discrepancies, was found to yield advantageous outcomes through the implementation of precise co-registration or traditional rectification techniques. The author conducted extensive research [22] that demonstrates the utilization of remote sensing methods in conjunction with geographic information systems (GIS) to map and monitor the risk of landslides in an Indian study area located in the Himalayas region. The study on how to estimate the danger of landslides using GIS data was presented in reference [23]. The researcher selected Chamoli-Joshi-math, located in the Himalayas region, as the focal point for this study. Instead of engaging in the study of RS images, the researchers collected satellite data, rainfall data, field observations, and other relevant sources. Nevertheless, this leads to inadequate evaluations and an inefficient approach to assessing the danger of landslides. A landslide detection technique based on RS image processing was developed in [24]. A hybrid system was presented, which incorporated object-oriented image analysis (OOIA), case-based reasoning (CBR), and a genetic algorithm (GA). An alternative approach to landslide detection, akin to the one described in [24], is demonstrated in [25]. By integrating two machine learning algorithms and a feature selection methodology, a semi-automatic framework was developed for the Three Gorges of China region. Their findings revealed three categories: (1) the presence of holes inside the landslide, (2) the removal of remote portions, and (3) the use of a hand-operated digitizing technique to illustrate closed envelope curves for landslide targets. The author conducted a study in [26] to examine the potential of remote sensing in facilitating quantitative estimates of landslide threats on a regional level, particularly in situations where data availability is limited. The landslide susceptibility and risk were evaluated using an automated classification technique on a multi-temporal landslide inventory generated from a 30-year time series of satellite TV for PC remote sensing data. One limitation of this approach is that the temporal component of landslide hazard can only be computed in the presence of a multi-temporal stock. The authors of [27] introduced the latest automated approach that utilizes multi-temporal remote sensing imagery to identify landslides. The approach for distinguishing patches was developed using the Deep Convolution Neural Network (DCNN) technology, which is specifically built for retrieving locations with a high degree of exchange. The proposed framework for multi-level extraction

and filtering includes the elimination of inappropriate locations, continual identification of landslides, and the optimization of top detection fees while minimizing false alarm costs. Nevertheless, a potential limitation of this methodology is the exclusion of some landslide locations from the landslide detection process, hence requiring further enhancements in terms of robustness and accuracy. In a previous study [28], introduced alternative methodologies that depend solely on remote sensing snapshots. The landslide locations on the Kii Peninsula were categorized by analyzing COSMO-Sky Med pictures taken before and after the landslides occurred. This study investigated the efficacy of utilizing differential back-scattering coefficients and intensity correlation for the detection of landslides. The speckle-noise dis-count approach was also evaluated using various window sizes. Nevertheless, this work unveiled some further limitations, such as constrained analysis, insufficient satellite data, and disparate acquisition timings of optical and SAR pictures, potentially leading to inaccurate detections. The hybrid approaches for landslide detection were further developed by the authors in [29], who utilized two established techniques, namely susceptibility analysis and change detection thresholding. The researchers conducted a quantitative analysis of the technique and asserted that it was more precise. Nevertheless, this methodology is limited to pixels with low resolution, whereas pixels with greater resolution are not taken into consideration. In the identification of landslides, a recent study [30] employed multi-scale picture segmentation and machine learning techniques. The researchers suggested a comprehensive approach for identifying landslides, which used item-based image analysis (OBIA) along with other machine learning techniques, including a multilayer perception neural network (MLP-NN), random forest (RF), and logistic regression (LR). The introduction of the multi-scale segmentation approach before the utilization of device learning algorithms. To achieve success and dependability, it is important to improve both the segmentation and classification phases through the use of mathematical principles and probability concepts.

In [31], a novel approach for landslide detection using LiDAR-derived data was introduced, which is based on OBIA. A framework was developed including many ideas such as the development of derivatives for digital elevation models (DEMs), segmentation at multiple resolutions, classification using SVMs, and post-processing techniques for improving the obtained results. Nevertheless, the author posits that the implementation of the OBIA approach remains a formidable obstacle in the realm of agricultural landslide detection. The imprecise classification might be attributed to the restricted visibility of topography in forested areas and the absence of high-resolution digital elevation model (DEM) data during the examination of landslides. Their detection approach was ineffective in accurately and comprehensively identifying the landslide. The utilization of machine learning and deep learning methodologies was developed to identify landslides by leveraging publically accessible resources [32]. The data about landslides was gathered, encompassing geological, topographic, and rainfall-related information. The classifiers used were SVM, random forest, logistic regression, and CNN. The absence of suitable computer vision techniques hindered the accuracy performance. In [33], a landslide prediction approach was introduced that utilizes improved principal component analysis (PCA) and least-squares supports vector regression (LSSVR) model. The purpose of this technique is to reduce the computational complexity and achieve a balance between the model's ability to generalize and learn. Nevertheless, the efficiency of this technique is constrained by the absence of RS picture pre-processing and ROI extractions. In their study, the authors of reference [34] included two distinct road components, namely road profile and road aspect, to enhance the precision of landslide susceptibility mapping. This was achieved by considering the influence of landslide movement direction on the road. A random forest classifier was utilized

to identify landslides on a provided dataset. To evaluate the efficacy of U-Net and machine learning algorithms in the context of automated landslide detection in the Himalayas, two datasets were created [35]. A dataset consisting of 239 samples was obtained from six training zones and one testing zone to evaluate the performance of the fully convolutional U-Net model, random forest, SVM, and KNN classifiers. The limited sample size did not provide sufficient evidence for the scalability of the proposed classifiers. The performance of accuracy is constrained as a result of inadequate computer vision algorithms. A recent study conducted by [36] examined the vulnerability of landslides and the geographical variations within the Qinghai-Tibetan Plateau (QTP) region. The study employed five different classifiers, including SVM, Random Forest, Logistic Regression, Naive Bayes, and Deep Neural Networks (DNN). Nevertheless, it is subject to the same limitations as [32–35].

2.2 Motivation

The recent studies presented on landslide prediction using the machine learning approaches suffer from various challenges. Many pattern recognition applications have been solved using deep learning methods. This study rejects these techniques because they are too complicated and unable to solve the special issues of RS image pre-processing, despite their speedy prediction and localization demands. Scalability and accuracy were difficult due to the study's small datasets. Datasets and studies on Indian landslide zones were scarce due to Chinese activity. Scalable landslide datasets are scarce in western India. Current approaches have higher prediction errors due to the lack of geometric correction and quality enhancement in input RS images. Poor landslide photo analysis, assessment problems, and difficulty locating landslide changes are among additional issues. Landslip prediction and severity ratings are lacking in the literature. To address the limitations of existing approaches for predicting landslide zones from RS images, a novel integrated framework based on efficient computer vision and soft computing techniques is suggested.

3 Proposed model

This section provides an overview of the design and methods employed in the proposed framework for semi-automatic landslide prediction and severity analysis. The block diagram in Fig. 1 illustrates the suggested methodology, which encompasses many stages including data collection, pre-processing, ROI extraction, features extraction, prediction, and severity analysis. The dataset that was obtained pertains to the landslide regions located in the western part of India. To examine the forecasting of landslides, the dataset was partitioned into two distinct subsets: training and testing. The initial stage of the proposed approach involves pre-processing, during which the bands R, G, Shortwave Infrared (SWIR), and near-infrared (NIR) are extracted, filtered, and used to calculate the Normalized Difference Vegetation Index (NDVI) for the input RS picture. The outcome of NDVI addresses the challenges of geometric and atmospheric corrections with denoising in the input RS image. The dynamic segmentation mechanism is applied to the pre-processed image to estimate the accurate ROI. We extracted texture and shape features from the ROI image to uniquely represent the variations in the RS image. The classifiers ANN and SVM are trained to predict the possibilities of landslide in the input RS image in the prediction step. Finally, if a landslide is projected, a severity analysis is undertaken for effective monitoring of future disasters.

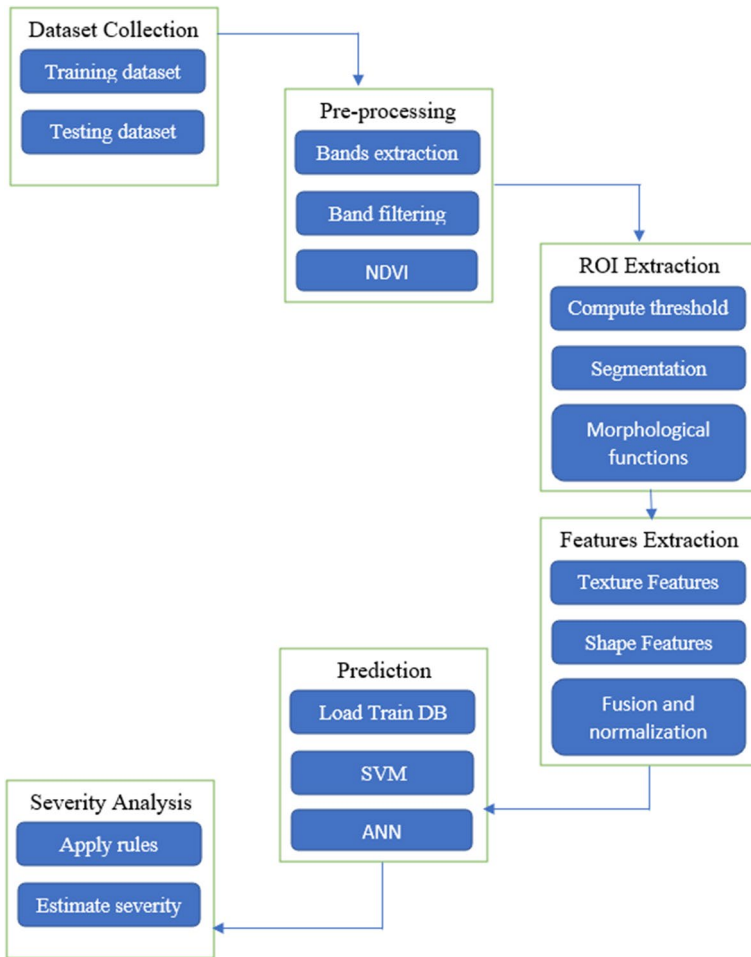


Fig. 1 Proposed real-time landslide prediction and severity analysis

3.1 Study area and dataset

The study has been conducted in the Konkan region located in western India. It spans around 100 km along the western coastlines of Maharashtra, Goa, and Karnataka, forming the Konkan area. The region in question is geographically bordered by the Western Ghats Mountain range to the east, the Arabian Sea to the west, the Daman Ganga River to the north, and the Aghanashini River to the south [37, 38]. The remote sensing (RS) samples were acquired specifically from the LISS-III satellite and have been categorized into two states, namely Maharashtra and Goa. The LISS-III pictures consist of four bands, namely R, G, SWIR, and NIR, each with different resolutions [42]. The collection of samples encompasses the landslide regions, encompassing both pre-landslide and post-landslide periods, spanning time series. Table 1 presents a comprehensive overview of the dataset that was gathered.

Table 1 Dataset specification

Regions	Pre-Landslides	Post-Landslides	Total samples
Maharashtra	355	1025	1380
Goa	355	978	1333
Western Region	710	2003	2713

- **Data collection method:** The major data collecting strategy employed in this study was the utilization of the observation technique to determine the location and get the image data.
- **Dataset Size:** As shown in Table 1, the dataset consists of a total of 2713 samples considering Maharashtra and Goa landslide regions.
- **Dataset Diversity:** The data was gathered in two distinct categories: pre-landslide and post-landslide. There is a varied range of data samples obtained for each class.
- **Data Validation Technique:** The dataset is partitioned using a k-fold cross-validation process, wherein 70% of the data samples are allocated for training purposes, while the remaining 30% are reserved for testing.

3.2 Pre-processing

The computer vision methods are designed in this work to perform the pre-processing, ROI extraction, and features extraction. Before that, we have corrected the input RS images geometrically and atmospherically for the LISS-3 sensor. The geometric correction has performed using the control points in the ERDAS tool. The Chavez radiometric correction technique applied on input RS image to suppress the atmospheric effects. After that, we extract the bands such as visible NIR and visible R bands from the corrected RS image to perform the NDVI. The NDVI pre-processing step has applied to correct the geometric regions, water, and vegetation further. Below steps shows the functionality of the pre-processing phase.

The input RS picture, denoted as S , was obtained from the LISS-3 satellite inside the designated research region. The original geometric and atmospheric effects were adjusted for each RS picture S in the collection. Subsequently, band extraction and NDVI computation were conducted utilizing Eqs. (1) and (2). The NDVI of the S is calculated by utilizing the spectral bands R (3) and NIR (4).

$$R = double(S(:, :, 3)) \quad (1)$$

$$NIR = double(S(:, :, 4)) \quad (2)$$

After extracting the 2D picture bands, we employed 2D median filtering to reduce noise in the image. To reduce noise from adjusted bands, the median filtering approach is employed. The algorithm for 2D median filtering operates by iteratively traversing the picture, replacing each pixel with the median value of the next pixel. The design of the neighbor is contingent upon the dimensions of the window. The present study used a window size of a 3-by-3 neighborhood. Equations (3) and (4) shows the median filtering of R and NIR bands.

$$R1(i, j) = median\{R(i, j) | (i, j) \in w\} \quad (3)$$

$$NIR1(i, j) = median\{NIR(i, j) | (i, j) \in w\} \quad (4)$$

where, $R1$ and $NIR1$ is outcome of median filtering and w is the size of window. Finally, the we computed the NDVI by using Eq. (5).

$$NDVI = \frac{(NIR1 - R1)}{(NIR1 + R1)} \quad (5)$$

The visual outcomes for the above steps are shown in Figs. 2 and 3 for two sample RS images 1 and 2 respectively. The input RS picture in Figs. 2 and 3 is designated as Coloured IR (CIR). The geometric and atmospheric adjustments have already been applied to this CIR picture. The visible red and NIR bands were extracted from the CIR picture. The aforementioned bands encompass the intrinsic noise elements that are mitigated with the application of median filtering. The NDVI picture has been generated by applying filters to the NIR and red bands.

3.3 Dynamic segmentation

This step takes the input NDVI image to locate the extract ROI for further analysis. The binary segmentation strategy employed in this study was the basic dynamic threshold-based method. The graythresh MATLAB function in Eq. (6) is used to calculate the dynamic threshold for each input NDVI picture. The rough ROI is retrieved from the NDVI in binary form based on the threshold value.

$$t = \text{graythresh}(NDVI) \quad (6)$$

Then, to estimate the ROI, the below steps are performed for NDVI of size $m \times n$ using Eq. (7).

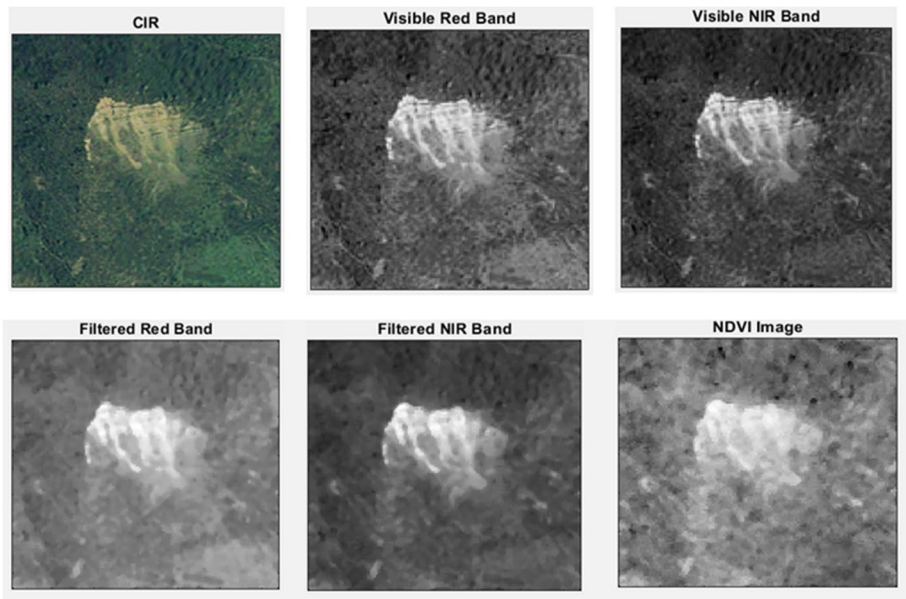


Fig. 2 Outcomes for the pre-processing of RS image1

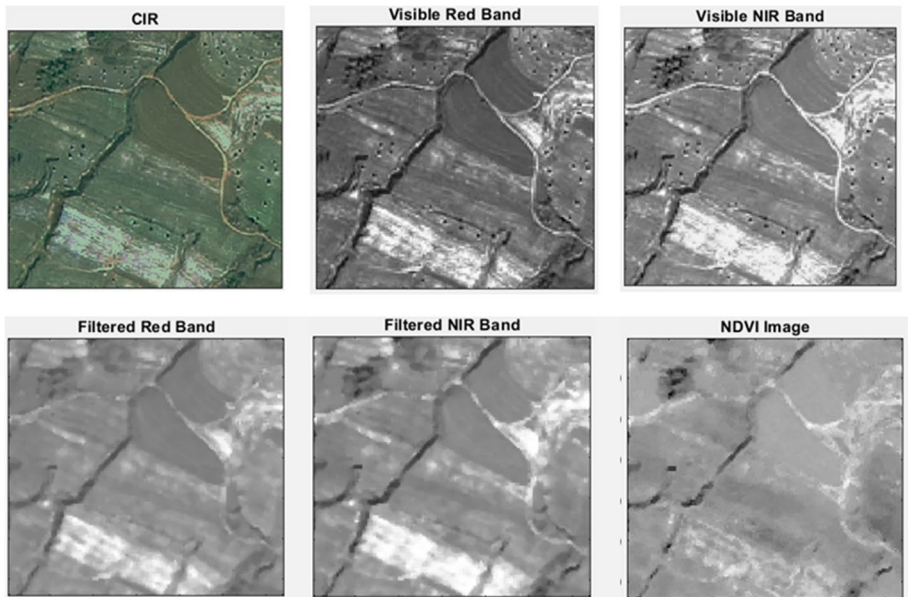


Fig. 3 Outcomes for the pre-processing RS image 2

$$ROI = (NDVI(i,j) > t), i = 1,2, \dots, m, j = 1,2, \dots, n \quad (7)$$

The ROI image may contain unwanted objects. Therefore, to refine the ROI output, we applied morphological operations. The morphological disc structuring element is created with its radius set to 3. This structural element plays a vital role in the morphological close operation. The morphological closure operation is executed using the result of the structural element (SE) function. The process of morphological close operation involves a sequential dilatation followed by erosion, whereby the same structural element is utilized for both operations. The steps are summarised in Eqs. (8) and (9) below.

$$SE = strel(ROI, 3) \quad (8)$$

By employing the element SE's structure, we enhance the existing ROI picture by the morphological close operation, resulting in the creation of the ultimate ROI.

$$ROI = imclose(ROI, SE) \quad (9)$$

Figure 4 shows the dynamic ROI extraction for two input samples shown in Figs. 2 and 3. As the outcome shows that core areas in the input RS images are affected by the landslide. Extraction of ROIs enables the removal of undesirable areas of RS images, which improves prediction accuracy.

3.4 Hybrid features extraction

Handcrafted features such as texture and shape features are widely used across different image processing applications. In this research, we retrieved texture and form features to estimate the distinct properties of the segmented ROI pictures of the input RS image.

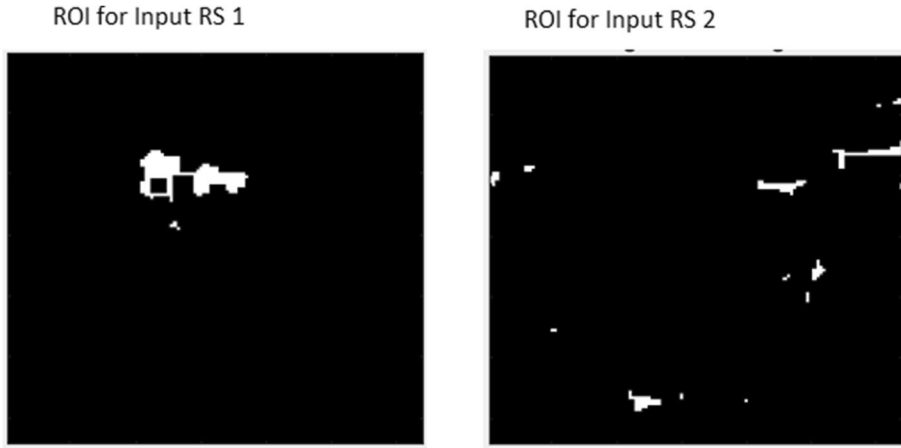


Fig. 4 ROI outcomes illustrations for two RS images

In image processing, the texture of an image may be described as the spatial variation of pixel brightness intensity. Texture is the primary word employed to delineate items or concepts within a given image. Consequently, we chose specific texture characteristics to accurately identify the landslide areas (if present) in the input ROI picture. As the texture features estimate the spatial variations in ROI image, temporal variations or characteristics are also essential for accurate prediction. Therefore, shape features are extracted to represent the temporal variations in the input ROI image.

i) Spatial Variations: The spatial variations from the input ROI images are estimated using the texture features. The texture features are extracted using Gray Level Co-occurrence Matrix (GLCM) and statistical features. The GLCM element for the input ROI image is defined using the GLCM function. Using that GLCM element, we have extracted the contrast (c), energy (e), homogeneity (h), and correlation (r) features using Eqs. (10) to (17) respectively. Let, g is the GLCM matrix and m and n represents the height and width of the ROI image.

$$c = \sum_{i=0}^{m-1} \sum_{j=0}^{n-1} |i - j|^2 g_{ij} \tag{10}$$

$$e = \sum_{i=0}^{m-1} \sum_{j=0}^{n-1} \frac{g_{ij}}{1 + |i - j|^2} \tag{11}$$

$$h = \frac{1}{\sigma_x \sigma_y} \sum_{i=0}^{m-1} \sum_{j=0}^{n-1} (i - j) g_{ij} - \mu_x \mu_y \tag{12}$$

where, the homogeneity elements such as $\mu_x, \mu_y, \sigma_x, \sigma_y$ are computed by:

$$\mu_x = \sum_{i=0}^{m-1} \sum_{j=0}^{n-1} g_{ij} \tag{13}$$

$$\mu_y = \sum_{j=0}^{n-1} \sum_{i=0}^{n-1} g_{ij} \tag{14}$$

$$\sigma_x^2 = \sum_{i=0}^{m-1} (i - \mu_x)^2 \sum_{j=0}^{n-1} g_{ij} \tag{15}$$

$$\sigma_x^2 = \sum_{j=0}^{n-1} (j - \mu_x)^2 \sum_{i=0}^{m-1} g_{ij} \tag{16}$$

Finally, the correlation feature is computed as:

$$r = \sum_{i=0}^{m-1} \sum_{j=0}^{n-1} g_{ij}^2 \tag{17}$$

After extraction of four GLCM features, we computed the statistical features such as mean, standard deviation, variance, bias, percentiles, and median. A total of 10 texture features are extracted from the input ROI image of size 1×10 .

ii) Temporal Variations: We retrieved the form characteristics to estimate the temporal fluctuations in the input ROI picture. Geometric moment invariance is an appropriate method for representing the shape properties of the ROI picture. Total 8 geometric invariance features are extracted using the first order $(f_{00}, f_{10}, f_{01}, f_{11})$ second-order (f_{12}, f_{21}) , and third-order (f_{13}, f_{31}) moment invariants as mentioned in the below Eqs. (18) to (25).

$$f_{00} = \sum_{i=1}^m \sum_{j=1}^n ROI(i, j) \tag{18}$$

$$f_{10} = \sum_{i=1}^m \sum_{j=1}^n iROI(i, j) \tag{19}$$

$$f_{01} = \sum_{i=1}^m \sum_{j=1}^n jROI(i, j) \tag{20}$$

$$f_{11} = \sum_{i=1}^m \sum_{j=1}^n (i - \bar{i})(j - \bar{j})ROI(i, j) \tag{21}$$

$$f_{12} = \sum_{i=1}^m \sum_{j=1}^n (i - \bar{i})(j - \bar{j})^2ROI(i, j) \tag{22}$$

$$f_{21} = \sum_{i=1}^m \sum_{j=1}^n ((i - \bar{i}))^2(j - \bar{j})ROI(i, j) \tag{23}$$

$$f_{13} = \sum_{i=1}^m \sum_{j=1}^n ((i - \bar{i}))^2(j - \bar{j})^2ROI(i, j) \tag{24}$$

$$f_{31} = \sum_{i=1}^m \sum_{j=1}^n ((i - \bar{i}))^3ROI(i, j) \tag{25}$$

Where, $\bar{i} = \frac{f_{10}}{f_{00}}$ and $\bar{j} = \frac{f_{01}}{f_{00}}$ are the coordinates of the object centroid.

iii) Normalization: The texture features (1×10) and shape features (1×8) combined together and formed the hybrid feature F of size 1×18 . As their significant variations among the extracted features, we opted for the scaling of such feature in particular range

of 0 to 1 using the min-max normalization technique. The normalized feature vector \hat{F} is produced using Eq. (26).

$$\hat{F} = \frac{(F - \min(F))}{(\max(F) - \min(F))} \quad (26)$$

3.5 Prediction

Two distinct classifiers, namely ANN and SVM, were trained to predict the likelihood of landslides based on the test RS sample. The artificial neural network classifier was built using a training dataset with 10 hidden layers. A back-propagation neural network was employed to learn 70% of the dataset. Only 30% of the test samples were utilized for prediction. We developed a multiclass SVM utilizing the 10-fold cross-validation technique. SVM training, similar to ANN, involves training on 70% of the training dataset and making predictions on 30% of the test samples. The architectural details about ANN and SVM are provided below.

- **ANN:** ANN is composed of several layers, with each layer serving a distinct purpose. As the intricacy of the model escalates, the quantity of layers likewise escalates, thereby earning the designation of a multi-layer perceptron. ANN in its most pristine state consists of three layers: the input layer, the hidden layer, and the output layer. The input layer is responsible for receiving input signals and transmitting them to the subsequent layer. Ultimately, the output layer generates the ultimate prediction. It is important to note that ANN, similar to machine learning algorithms, must undergo training using training data before approaching a specific problem. The input layer receives the initial information and passes it on to the hidden layers, which give weights to each input at random. After biasing each input neuron, the activation function gets the weighted sum of weights and bias. The Activation Function activates nodes for feature extraction and calculates output. This is referred to as forward propagation. After comparing the output model to the original output, the error is calculated and weights are adjusted in backward propagation to reduce the error. This procedure repeats for a predetermined number of epochs. The model weights are adjusted, and the forecast is complete.
- **SVM:** SVM is a widely used algorithm in Supervised Learning, capable of handling both Classification and Regression problems. However, it is primarily used for solving classification problems in machine learning. Similar to a data scientist, the SVM algorithm aims to generate an optimal line or decision boundary to effectively divide n-dimensional space into distinct classes. This allows for easy categorization of future data points. This optimal decision boundary is referred to as a hyperplane. Support Vector Machines select the most crucial points or vectors to construct the hyperplane. These extreme cases are known as support vectors, leading to the algorithm being referred to as SVM. SVM may be classified into two categories: non-linear and linear. The Linear SVM is employed for data that can be categorized into two distinct groups using a single straight line. This type of data is referred to as linearly separable data, and the classifier used for this purpose is known as the Linear SVM classifier. The Non-Linear SVM is employed for data that is not linearly separated. This implies that if a dataset cannot be classified using a straight line, it is referred to as non-linear data. The classifier utilized in such cases is known as the Non-linear SVM classifier.

Algorithm summarizes the entire procedure of the landslide prediction using above steps.

Algorithm Landslide prediction

Input:

S: Input RS image

T: Train DB

C: Training Classes

Output:

P: Prediction result

1. Acquisition of RS image *S*
2. Extraction of *R* and *NIR* images, $R, NIR \in S$
3. Apply median filtering on *R* and *NIR* images using Eq. (3) & Eq. (4)
4. Compute NDVI using Eq. (5).
5. $roi \leftarrow getSeg(NDVI)$
6. If ($roi \neq NULL$)
7. $f1 \leftarrow getTexture(roi)$
8. $f2 \leftarrow getShape(roi)$
9. $F \leftarrow [f1, f2]$
10. Normalize *F* using Eq. (26)
11. Else
12. Discard *S*
13. End
14. $P \leftarrow classify(F, T, C)$
15. Return (*P*)

3.6 Severity analysis

Like any disease severity analysis, the severity estimation of the predicted landslides facilitates the effective and easy monitoring of future disaster conditions. In this research, we used the normalized hybrid feature vector to assess the severity of projected landslides. The goal of this severity study is to evaluate the likelihood of landslides in that specific location. We calculated three types of landslide chances using expert analysis: lower probability, average possibility, and severe potential. Table 2 displays the top and lower ranges determined by the expert's study. Lower and upper boundaries are set by confirming maximum accuracy with field specialists.

4 Experimental procedure

The proposed model was built with the help of the well-known image processing tool MATLAB, as previously stated. The implementation was carried out using the Windows 10 operating system, 8 GB of RAM, and an Intel I5 CPU. The performance of the western area of India had examined using the dataset presented in the preceding portion of this article. The whole dataset comprises 2713 RS imagery samples collected from the landslide zones of Maharashtra and Goa. This dataset has been separated into two parts: training samples (70%) and testing samples (30%). Following the categorization of 30% of the samples, we have assessed the five performance measures, which include accuracy, f1-score (precision), recall (recall), and specificity (specificity). We did this by examining the confusion matrix parameters. A large number of studies have made the formulae for calculating these parameters widely available. Spatial features (SF), temporal features (TF), and normalized hybrid features (NHF) are used in this part to conduct a comparative study of SVM and ANN classifiers (HF).

5 Results

Figures 5, 6, 7, 8 and 9 show the results for the accuracy, F1-score, precision, recall, and specificity parameters, as well as their corresponding values.

Figure 6 shows outcomes of prediction accuracy using the ANN and SVM with SF, TF, and normalized HF features. The ANN classifier has superior accuracy performance compared to the SVM classifier. The primary factor contributing to the increased accuracy of the ANN is its effective resolution of non-linear issues in comparison to the SVM classifier. The kernel function plays a crucial role in SVM as it employs nonlinear mapping techniques to achieve linear separability of the input. ANN employs multi-layer connections and numerous activation functions to address nonlinear problems. The performance of the ANN in prediction is enhanced when compared to the SVM classifier, irrespective of the type of features utilized for training and testing. The F1-score performance in Fig. 6, the precision rate in Fig. 7, the recall rate in Fig. 8, and the specificity rate in Fig. 9 all indicate that the ANN classifier surpassed the SVM classifier in terms of accuracy performance while employing various features such as SF, TF, and normalized HF. The higher accuracy for ANN is 93.38% and SVM is 92.29%. The maximum F1-score using ANN is 93.54% and using SVM is 90.1%. The maximum precision rate using ANN is 92.65% and

using SVM is 89.25%. The maximum recall rate using ANN is 94.45% and using SVM is 90.96%. The maximum specificity rate using ANN is 93.46% and using SVM is 92.28%. The backpropagation neural network delivered landslide prediction performances approximately 2+ % higher than the multiclass SVM classifier in our study

Apart from the investigation of the classifier's performances, the outcomes in Figs. 5, 6, 7, 8 and 9 also demonstrate the analysis of the various features of SF, TF, and normalized HF. We investigated the texture features (SF), geometric moment features (TF), and the hybrid feature vector with normalization HF to access the impact of using them on the overall prediction performances. From the achieved outcomes, it is observed that normalized HF features produced improved prediction results compared to the individual SF and TF features. The obvious reason for this lack of sufficient information about the landslide regions (pre-landslide and post-landslide). Either TF or SF features missing while utilizing them for the classification which leads to poor prediction outcomes. Among the SF and TF, SF features produced a higher prediction performance compared to TF. However, combining and normalizing the SF and TF has improved the overall prediction performances approximately by 8%. Table 3 shows the comparative study for SVM and ANN using the normalized HF. The results concluded that the proposed model using the ANN classifier and normalized HF delivered improved performances for landslide prediction compared to other approaches.

Table 4 shows an analysis of the ablation study in this research where we have analyzed the shape, texture, and hybrid features analysis to claim the impact of combining the shape and texture features and their normalization. Ablation research examines the efficacy of an AI system by selectively eliminating specific components to comprehend the individual impact of each component on the overall system. We first analyzed the TF for landslide detection and analyzed its performance. Then the SF for the landslide detection and analyzed its performance. Finally, the TF and SF combined into HF with the normalization. It shows a significant performance improvement in landslide prediction performances using the HF.

6 Discussions

Finally, we presented the comparative study with similar state-of-the-art methods using the proposed dataset in terms of prediction accuracy, F1 score, and average prediction time. The average prediction time for each method is estimated after executing the 25 test samples. Table 4 demonstrates the outcome of the comparative study with similar methods. We have selected 4 recent methods for the comparative study such as Li et al. [33], Ye et al. [34], Meena et al. [35], Sajadi et al. [36], Ma et al. [39], Hussain et al. [40], and Sun et al. [41]. Table 5 claims that the proposed model using ANN delivered improved accuracy and F1-score performances for the landslide prediction with minimum prediction time compared to existing recent methods. The primary reasons for

Table 2 Parameters for the landslide severity analysis

Landslide severity	Lower bound	Upper bound
Lower possibility	0	0.25
Average possibility	0.26	0.5
Severe possibility	0.51	1.0

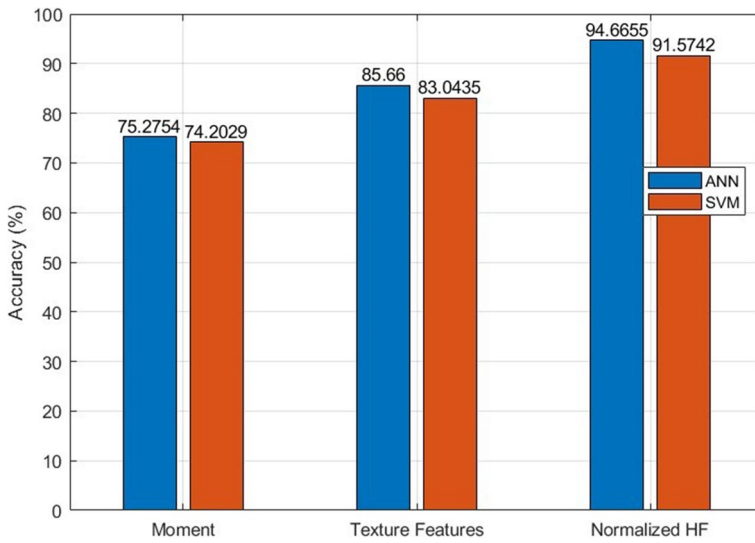


Fig. 5 Prediction accuracy analysis using different classifiers and features

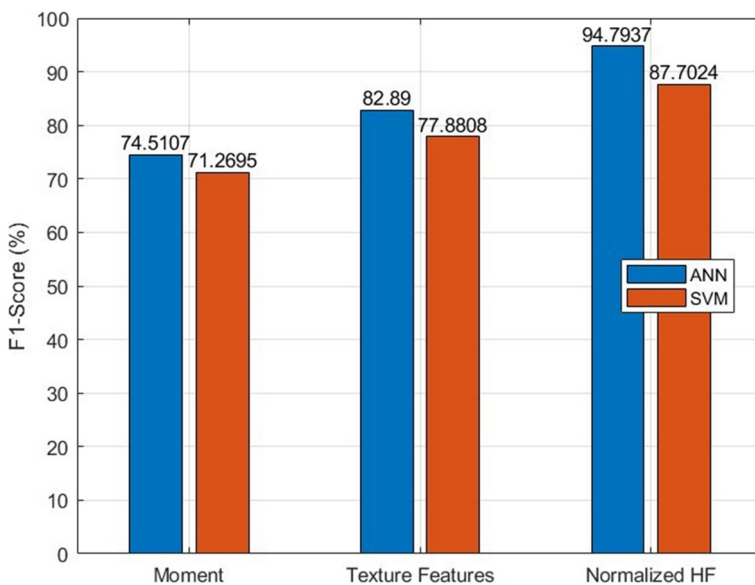


Fig. 6 Prediction F1-score analysis using different classifiers and features

performance improvement are the inclusion of a diverse set of computer vision features, their hybridization, and their normalization. It overcomes the additional classification errors at training, testing, and validations and improves the overall prediction accuracy of the proposed model compared to all existing methods. Recently, we have utilized the deep learning as well in [42].

The suggested model’s outputs for landslide prediction are summarized as follows.

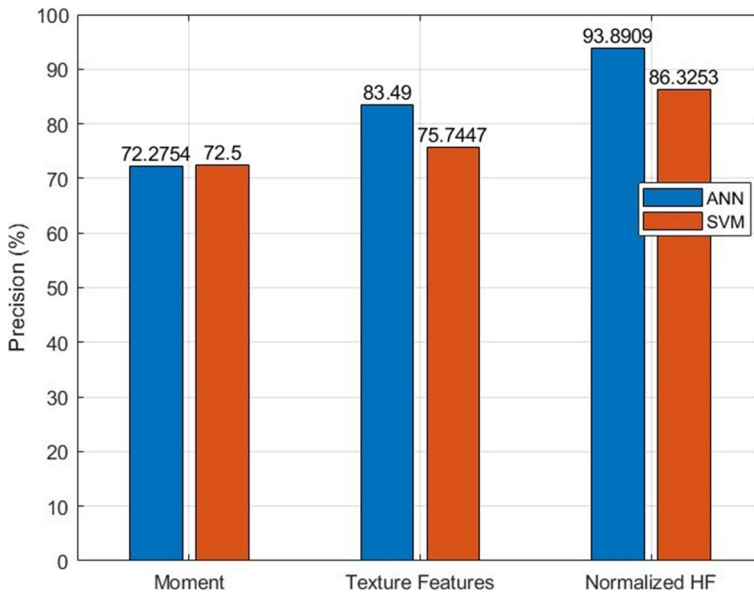


Fig. 7 Precision analysis using different classifiers and features

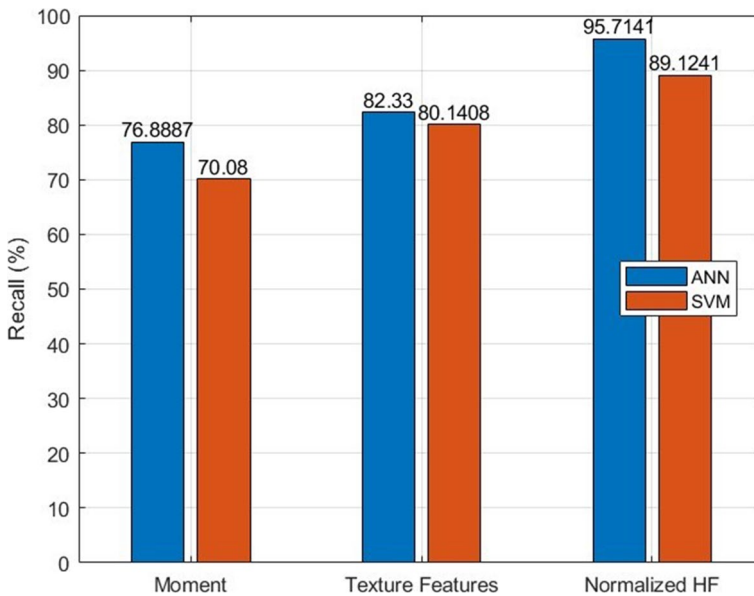


Fig. 8 Recall analysis using different classifiers and features

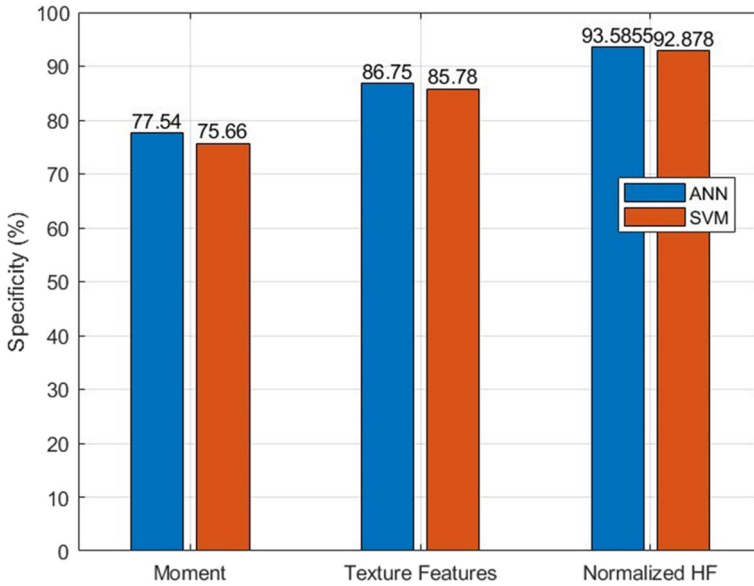


Fig. 9 Specificity analysis using different classifiers and features

- Improving the quality of RS images before the feature extraction using the R and NR bands helps to estimate the appropriate features in the proposed model.
- Extracting the texture and shape features followed by its normalization helps to improve the landslide prediction accuracy in the proposed model over the existing methods.
- Evaluating the model using the ANN and SVM classifiers shows a reduction in the classification errors.

Although the proposed model shows better accuracy for the landslide prediction, the challenges related to security from the malicious users remain unexplored. Recently, studies like [43–45] have discussed the security issues for the different types of data and their solutions. Thus, it is a potential limitation of the proposed study.

Table 3 Comparative analysis of SVM and ANN results using normalized HF

Measures	SVM	ANN
Accuracy (%)	92.29	93.38
F1-score (%)	90.1	93.54
Precision (%)	89.25	92.65
Recall (%)	90.96	94.45
Specificity (%)	92.87	93.58

Table 4 Analysis of different feature extraction methods for ablation study

Measures	TF	SF	Normalized HF
Accuracy (%)	87.44	79.85	93.38
F1-score (%)	87.25	79.54	93.54
Precision (%)	85.94	78.35	92.65
Recall (%)	88.61	80.77	94.45
Specificity (%)	86.35	78.98	93.46

Table 5 State-of-the-art comparative analysis

Methods	Accuracy (%)	F1-score (%)	Average Prediction Time (Seconds)
Li et al. [33]	84.67	83.23	2.34
Ye et al. [34]	86.83	86.42	2.51
Meena et al. [35]	85.94	84.39	2.78
Sajadi et al. [36]	87.93	86.03	2.29
Ma et al. [39]	89.34	89.09	2.58
Hussain et al. [40]	88.45	87.57	2.67
Sun et al. [41].	88.67	88.03	2.46
Proposed	93.38	93.54	2.17

7 Conclusion

This study presents a unique framework for the processing of real-time RS images, intending to predict the likelihood of landslides and conduct severity assessments. The system was specifically developed to mitigate the limitations of current methodologies, which include the absence of a scalable dataset for Indian landslides, the inability to effectively handle RS image corrections and denoising, localization of landslide ROI, and analysis of severity. The present study employed state-of-the-art computer vision and soft computing technologies to develop a straightforward but efficient framework. The data about the western regions of India was obtained directly from the Bhuvan LISS-3 satellite network. Before denoising and calculating NDVI, the collected RS images underwent correction for geometric and atmospheric imperfections. A dynamic segmentation method was employed to extract the ROI from the NDVI image. The development of hybrid feature vectors aims to enhance the accuracy of predictions by integrating both temporal and spatial fluctuations. The simulation results demonstrated that the suggested model exhibited a 6% enhancement in prediction accuracy compared to current research, and a 5% improvement in F1 score compared to prior methodologies. Despite the longer training and testing time of deep learning models, we suggest employing deep learning to improve prediction in future research. In addition, another crucial research direction for this study is determining the precise location of the anticipated landslide zone.

Funding None.

Data availability Data sharing not applicable to this article as no datasets were generated or analyzed during the current study.

Declarations

Ethical approval This article does not contain any studies with human participants performed by any of the authors.

Conflict of interest All authors declares that they has no conflict of interest.

References

- Guzzetti F, Reichenbach P, Cardinali M, Galli M, Ardizzone F (2005) Probabilistic landslide hazard assessment at the basin scale. *Geomorphology* 72:272–299. <https://doi.org/10.1016/j.geomorph.2005.06.002>
- Perkins S (2012) Death toll from landslides vastly underestimated. <http://www.nature.com/>, <http://www.emdat.be/database>. Accessed 15 Jan 2022
- Nguyen TL (2008) Landslide susceptibility mapping of the mountainous area in a Luoi District. Thua Thien Hue Province, Vietnam Vrije Universiteit Brussel
- de Lito FLR, Carvalho Vieira B (2012) Mapping of risk and susceptibility of shallow-landslide in the city of São Paulo, Brazil. *Geomorphology* 169–170:30–44. <https://doi.org/10.1016/j.geomorph.2012.01.010>
- Pradhan B (2010) Landslide susceptibility mapping of a catchment area using frequency ratio, fuzzy logic and multivariate logistic regression approaches. *J Indian Soc Remote Sens* 38(2):301–320. <https://doi.org/10.1007/s12524-010-0020-z>
- Remondo J, Bonachea J, Cendrero A (2008) Quantitative landslide risk assessment and mapping on the basis of recent occurrences. *Geomorphology* 94(3–4):496–507. <https://doi.org/10.1016/j.geomorph.2006.10.041>
- Mahajan HB, Uke N, Pise P et al (2022) Automatic robot Manoeuvres detection using computer vision and deep learning techniques: a perspective of internet of robotics things (IoRT). *Multimed Tools Appl*. <https://doi.org/10.1007/s11042-022-14253-5>
- Aksoy B, Ercanoglu M (2012) Landslide identification and classification by object-based image analysis and fuzzy logic: An example from the Azdavay region (Kastamonu, Turkey). *Computers, Geosciences* 38(1):87–98. <https://doi.org/10.1016/j.cageo.2011.05.010>
- Tien Bui D (2012) Modeling of rainfall-induced landslide hazard for the Hoa Binh, province of Vietnam. Norwegian University of Life Sciences. Ph.D Thesis
- Pradhan B, Lee S, Buchroithner M (2010) A GIS-based back-propagation neural network model and its cross-application and validation for landslide susceptibility analyses. *Comput Environ Urban Syst* 34:216–235. <https://doi.org/10.1016/j.compenvurbys.2009.12.004>
- Arabameri A, Saha S, Roy J, Chen W, Blaschke T, Tien Bui D (2020) Landslide susceptibility evaluation and management using different machine learning methods in the Gallicash River Watershed, Iran. *Remote Sens* 12(3):475. <https://doi.org/10.3390/rs1203047>
- Sezer E, Pradhan B, Gokceoglu C (2011) Manifestation of an adaptive neuro-fuzzy model on landslide susceptibility mapping: Klang Valley, Malaysia. *Expert Syst Appl* 38:8208–8219. <https://doi.org/10.1016/j.eswa.2010.12.167>
- Khanlari GR, Heidari M, Momeni AA, Abdilor Y (2012) Prediction of shear strength parameters of soils using artificial neural networks and multivariate regression methods. *Eng Geol* 131–132:11. <https://doi.org/10.1016/j.enggeo.2011.12.006>
- Lee S, Hwang J, Park I (2013) Application of data-driven evidential belief functions to landslide susceptibility mapping in Jinbu, Korea. *Catena* 100:15–30. <https://doi.org/10.1016/j.catena.2012.07.014>
- Lee S, Min K (2001) Statistical analysis of landslide susceptibility at Yongin, Korea. *Environ Geol* 40(9):1095–1113. <https://doi.org/10.1007/s002540100310>
- Pradhan B (2013) A comparative study on the predictive ability of the decision tree, support vector machine and neuro-fuzzy models in landslide susceptibility mapping using GIS. *Comput Geosci* 51:350–365. <https://doi.org/10.1016/j.cageo.2012.08.023>
- San BT (2014) An evaluation of SVM using polygon-based random sampling in landslide susceptibility mapping: the Candir catchment area (western Antalya, Turkey). *Int J Appl Earth Obs Geoinf* 26:399–412. <https://doi.org/10.1016/j.jag.2013.09.010>
- Hwang S, Guevarra IF, Yu B (2009) Slope failure prediction using a decision tree: a case of engineered slopes in South Korea. *Eng Geol* 104(1–2):126–134. <https://doi.org/10.1016/j.enggeo.2008.09.004>

19. Marjanović M, Kovačević M, Bajat B, Voženílek V (2011) Landslide susceptibility assessment using SVM machine learning algorithm. *Eng Geol* 123(3):225–234. <https://doi.org/10.1016/j.enggeo.2011.09.006>
20. Mohan A, Kumar B, Dwivedi R (2021) Review on remote sensing methods for landslide detection using machine and deep learning. *Trans Emerg Telecommun Technol* 32. <https://doi.org/10.1002/ett.3998>
21. Lacroix P, Zavala B, Berthier E, Audin L (2013) Supervised method of landslide inventory using Panchromatic SPOT5 images and application to the earthquake-triggered landslides of Pisco (Peru, 2007, Mw8.0). *Remote Sens* 5(6):2590–2616. <https://doi.org/10.3390/rs5062590>
22. Rai PK, Mohan K, Kumra VK (2014) Landslide hazard and its mapping using remote sensing and GIS. *J Sci Res* 58:1–133333
23. Chaturvedi P, Dutt V, Jaiswal B, Tyagi N, Sharma S, Mishra Sp, Dhar S, Joglekar P (2014) Remote sensing based regional landslide risk assessment. *Int J Emerg Trends Electr Electron* 2320–9569(10):135–140
24. Dou J, Chang K-T, Chen S, Yunus A, Liu J-K, Xia H, Zhu Z (2015) Automatic case-based reasoning approach for landslide detection: Integration of object-oriented image analysis and a genetic algorithm. *Remote Sens* 7(4):4318–4342. <https://doi.org/10.3390/rs70404318>
25. Li X, Cheng X, Chen W, Chen G, Liu S (2015) Identification of forested landslides using LiDAR data, object-based image analysis, and machine learning algorithms. *Remote Sensing* 7(8):9705–9726. <https://doi.org/10.3390/rs70809705>
26. Golovko D, Roessner S, Behling R, Wetzel H-U, Kleinschmit B (2017) Evaluation of remote-sensing-based landslide inventories for hazard assessment in Southern Kyrgyzstan. *Remote Sens* 9(9):943. <https://doi.org/10.3390/rs9090943>
27. Chen Z, Zhang Y, Ouyang C, Zhang F, Ma J (2018) Automated landslides detection for Mountain cities using Multi-temporal Remote sensing imagery. *Sensors* 18(3):821. <https://doi.org/10.3390/s18030821>
28. Konishi T, Suga Y (2018) Landslide detection using COSMO-SkyMed images: a case study of a landslide event on Kii Peninsula, Japan. *Eur J Remote Sens* 51(1):205–221. <https://doi.org/10.1080/22797254.2017.1418185>
29. Si A, Zhang J, Tong S, Lai Q, Wang R, Li N, Bao Y (2018) Regional landslide identification based on susceptibility analysis and change detection. *ISPRS Int J Geo-Information* 7(10):394. <https://doi.org/10.3390/ijgi7100394>
30. Tavakkoli Piralilou S, Shahabi H, Jarihani B, Ghorbanzadeh O, Blaschke T, Gholamnia K, Aryal J (2019) Landslide detection using multi-scale image segmentation and different machine learning models in the higher himalayas. *Remote Sens* 11(21):2575. <https://doi.org/10.3390/rs11212575>
31. Pawluszek K, Marczak S, Borkowski A, Tarolli P (2019) Multi-aspect analysis of object-oriented landslide detection based on an Extended Set of LiDAR-Derived Terrain features. *ISPRS Int J Geo-Information* 8(8):321. <https://doi.org/10.3390/ijgi8080321>
32. Wang H, Zhang L, Yin K, Luo H, Li J (2020) Landslide identification using machine learning. *Geosci Front*. <https://doi.org/10.1016/j.gsf.2020.02.012>
33. Li L, Cheng S, Wen Z (2021) Landslide prediction based on improved principal component analysis and mixed kernel function least squares support vector regression model. *J Mt Sci* 18:2130–2142. <https://doi.org/10.1007/s11629-020-6396-5>
34. Ye C, Wei R, Ge Y et al (2022) GIS-based spatial prediction of landslide using road factors and random forest for Sichuan-Tibet Highway. *J Mt Sci* 19:461–476. <https://doi.org/10.1007/s11629-021-6848-6>
35. Meena SR, Soares LP, Grohmann CH et al (2022) Landslide detection in the Himalayas using machine learning algorithms and U-Net. *Landslides*. <https://doi.org/10.1007/s10346-022-01861-3>
36. Sajadi P, Sang Y-F, Gholamnia M, Bonafoni S (2022) Evaluation of the landslide susceptibility and its spatial difference in the whole Qinghai-Tibetan Plateau region by five learning algorithms. *Geosci Lett* 9. <https://doi.org/10.1186/s40562-022-00218-x>
37. <https://bhuvan.nrsc.gov.in/home/index.php>. Accessed 21 Dec 2021
38. <https://www.usgs.gov/centers/eros/science/usgs-eros-archive-isro-resourcesat-1-and-resourcesat-2-liss-3>. Accessed 4 Dec 2021
39. Ma S, Chen J, Wu S, Li Y (2023) Landslide susceptibility prediction using machine learning methods: a case study of landslides in the Yinghu Lake Basin in Shaanxi. *Sustainability* 15(22):15836. <https://doi.org/10.3390/su152215836>
40. Hussain MA, Chen Z, Zheng Y, Zhou Y, Daud H (2023) Deep learning and machine learning models for landslide susceptibility mapping with remote sensing data. *Remote Sens* 15(19):4703. <https://doi.org/10.3390/rs15194703>

41. Sun D, Chen D, Zhang J, Mi C, Gu Q, Wen H (2023) Landslide susceptibility mapping based on interpretable machine learning from the perspective of geomorphological differentiation. *Land* 12(5):1018. <https://doi.org/10.3390/land12051018>
42. Varangaonkar P, Rode SV (2023) Lightweight deep learning model for automatic landslide prediction and localization. *Multimed Tools Appl* 82:33245–33266. <https://doi.org/10.1007/s11042-023-15049-x>
43. Mahajan HB, Junnarkar AA (2023) Smart healthcare system using integrated and lightweight ECC with private blockchain for multimedia medical data processing. *Multimed Tools Appl*. <https://doi.org/10.1007/s11042-023-15204-4>
44. Kadam MV, Mahajan HB, Uke NJ, Futane PR (2023) Cybersecurity threats mitigation in internet of vehicles communication system using reliable clustering and routing. *Microprocess Microsyst* 102:104926. <https://doi.org/10.1016/j.micpro.2023.104926>
45. Mahajan H, Reddy KTV (2023) Secure gene profile data processing using lightweight cryptography and blockchain. *Cluster Comput*. <https://doi.org/10.1007/s10586-023-04123-6>

Publisher's Note Springer Nature remains neutral with regard to jurisdictional claims in published maps and institutional affiliations.

Springer Nature or its licensor (e.g. a society or other partner) holds exclusive rights to this article under a publishing agreement with the author(s) or other rightsholder(s); author self-archiving of the accepted manuscript version of this article is solely governed by the terms of such publishing agreement and applicable law.